

# INTERACTION OF $\sim 9$ GeV PROTONS WITH NUCLEONS AND PHOTO-EMULSION NUCLEI †

This work was carried out by three groups of the Joint Institute for Nuclear Research, Dubna

- I. V. Beliaikov, Van Shu-fen', V. Glagolev, Dalkhazhav, L. Kirillova, P. Markov, R. Lebedev, K. Tolstov, E. Tsyganov, M. Shafranov, Jao Tsyng-se.
- II. B. Bannik, G. Bajatjan, I. Gramenitskij, M. Danysz, N. Kostanashvili, V. Lyubimov, A. Nomofilov, M. Podgoretskij, E. Skshipchak, D. Tuvdendorge, O. Shahulashvili.
- III. N. Bogachev, S. Bunyatov, T. Vishki, Yu. Merekov, V. Sidorov.

The emulsion stack, containing 100 pellicles of NIKFI-R photo-emulsion of  $450\mu$  thickness and  $10 \times 10 \text{ cm}^2$  surface was exposed in the Synchrophasotron of the High Energy Laboratory of the Joint Institute for Nuclear Research to the inner proton beam, accelerated to 8.7 GeV. The work was carried out by three groups, who investigated proton interaction with free and bound nucleons of photo-emulsion (groups II and III), mechanism of proton interaction with photo-emulsion nuclei (group I), generation of  $\pi^0$  mesons and "strange" particles (group II); besides that, an attempt was made to investigate proton diffraction scattering on photo-emulsion nuclei (group II).

## A. 9 GeV proton interaction with free and bound nucleons in photo-emulsion

Emulsion pellicles have been scanned along tracks of primary protons. 2366 cases of proton interaction with nuclei (scattering on the angle less than  $5^\circ$  was not included) in 871 m track length were found. The cases of primary proton interaction with free protons and protons bound in nuclei were separated on the basis of the following criteria:

- a) even number of the tracks;
- b) absence of an electron, emitted from the star centre;
- c) the range of the secondary particles, except protons from elastic  $p-p$  scattering, mesons and hyperons, should exceed 4 mm, which allows exclusion of interaction cases in which evaporation particles are present;
- d) the angles of the secondary particles emitted and their energy should not contradict the kinematics of proton collision with rest proton. The case was considered as proton collision with quasi-free neutron, if the star had odd number of tracks and satisfied (c) and (d) for selection of  $p-p$  events. 205 cases have been selected in this way, similar to  $p-p$  interactions, and 123 cases, similar to  $p-n$  interactions referred to below as  $p-p$  and  $p-n$  events. Assuming that the number of proton collisions with quasi-free

protons in the nucleus is equal to the number of collisions with quasi-free neutrons and excluding the cases of elastic  $p-p$  scattering, one may obtain as an approximate estimate of the cross-section of inelastic  $p-p$  interaction of 9 GeV the value  $\sim 30$  mb. The hydrogen content in emulsion was calculated by the data given in the papers <sup>1,2)</sup>. It follows from the papers <sup>3-12)</sup> and from the given estimate, that the cross-section of inelastic  $p-p$  interaction is practically unchanged in the interval from 1 to 9 GeV. The results <sup>13-15)</sup> relating to the cosmic rays, indicate that the cross-section of inelastic  $p-p$  interaction probably remains constant in the interval of higher energies.

From 205  $p-p$  events 17 cases were related to elastic  $p-p$  scattering on the hydrogen in emulsion. Due to the insufficiency of the statistics, differential cross-section of elastic  $p-p$  scattering cannot be estimated; it should be noted that in the majority of the cases the scattering angles in c.m.s. do not exceed  $20^\circ$ , which probably indicates the diffraction character of the scattering.

The registration efficiency of the cases of elastic scattering depends on the angle between the plane of scattering and the plane of the emulsion and must be evaluated in determining the total cross-section of elastic  $p-p$  scattering. The correction has been calculated for 39 cases, which in the sense of the registration efficiency are similar to the cases of elastic  $p-p$  scattering, and it turned out to be equal to  $1.5 \pm 0.2$ . The total cross-section of elastic  $p-p$  scattering at 9 GeV, taking into account the above-mentioned corrections and the background of quasi-elastic  $p-p$  scattering ( $\sim 20\%$ ), is  $\sigma_{p-p}^{el} = (10 \pm 5)$  mb. The comparison of this value with experimental data <sup>10)</sup> shows that the total cross-section of elastic  $p-p$  scattering at the energy range from 6 GeV to 9 GeV within the limits of the experiment errors does not change. The estimation of the total cross-section of  $p-p$  scattering at 9 GeV, obtained as the sum of elastic and inelastic cross-sections, leads to the value  $\sim 40$  mb.

Distributions  $N(n)$  and  $N(n_s)$  inelastic  $p-p$  events and  $p-n$  events according to the number of all tracks  $n$  and

† Appendix to Session 2. — Experimental II.

the number of fast particles  $n_s$  (i.e. particles with ionization  $I < 1.4 I_{plateau}$ ) are given in Table I.

The calculations made according to the statistical theory lead, at  $E = 8.7$  GeV, to  $\bar{n} = 3.3$  for  $p-p$  and  $\bar{n} = 3.0$  for  $p-n$ .

The comparison with the results of the papers<sup>10,12)</sup> indicates that the average number of charged particles emitted in  $p-p$  interactions increases rather slowly in the energy range of the incident proton from 3 GeV to 9 GeV. The mean number of charged shower particles emitted in  $p-p$  events at 9 GeV is less than the value  $\bar{n}_s = 3.4 \pm 0.1$  obtained for proton-nucleus interaction<sup>17)</sup>.

The angular distributions in the laboratory system of all charged particles and shower particles are given in Figs. 1, 2 and 3 where on the abscissa is plotted the cosine of the polar angle and on the ordinate the relative number  $f(\cos \theta)$  of particles, emitted in a given interval of  $\cos \theta$ .

The angular distributions of the charged particles from  $p-p$  and  $p-n$  events in the limits of the statistical errors coincide (Fig. 1). A half of the secondary particles is emitted in the cone with the angle  $19.0^\circ \pm 1.5^\circ$  for  $p-p$  events and  $17.0^\circ \pm 2.4^\circ$  for  $p-n$  events. The angular distributions of the prongs in inelastic  $p-p$  events for different  $n$  (Fig. 2) in the limits of the errors are not distinguishable.

If, in the centre of mass system, all the particles are relativistic ( $E \gg mc^2$ ) in the case of  $p-p$  events, in the laboratory system a half of the particles should emerge in the cone with the angle  $23^\circ$ . From the comparison of this value with the experimental value obtained it probably follows that there is present in the c.m.s. a number of relatively slow secondary particles. The angular distributions of

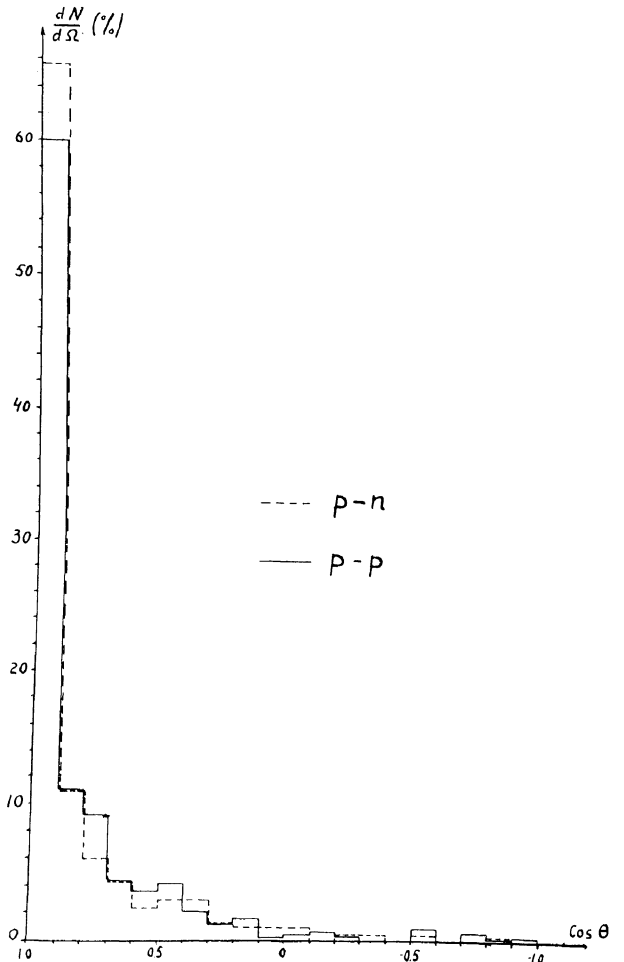


Fig. 1. The angular distributions of the charged secondary particles in  $p-p$  and  $p-n$  collisions.

TABLE I

	$p-p$		$p-n$	
	$N(n)$	$N(n_s)$	$N(n)$	$N(n_s)$
1	2	3	4	5
0	—	0	—	7
1	—	35	39	38
2	90	60	—	13
3	—	32	61	49
4	81	44	—	5
5	—	5	19	13
6	15	10	—	2
7	—	1	3	1
8	2	1	—	—
9	—	—	1	—
Mean number of tracks per star	$3.24 \pm 0.08$	$2.69 \pm 0.07$	$2.82 \pm 0.20$	$2.52 \pm 0.20$

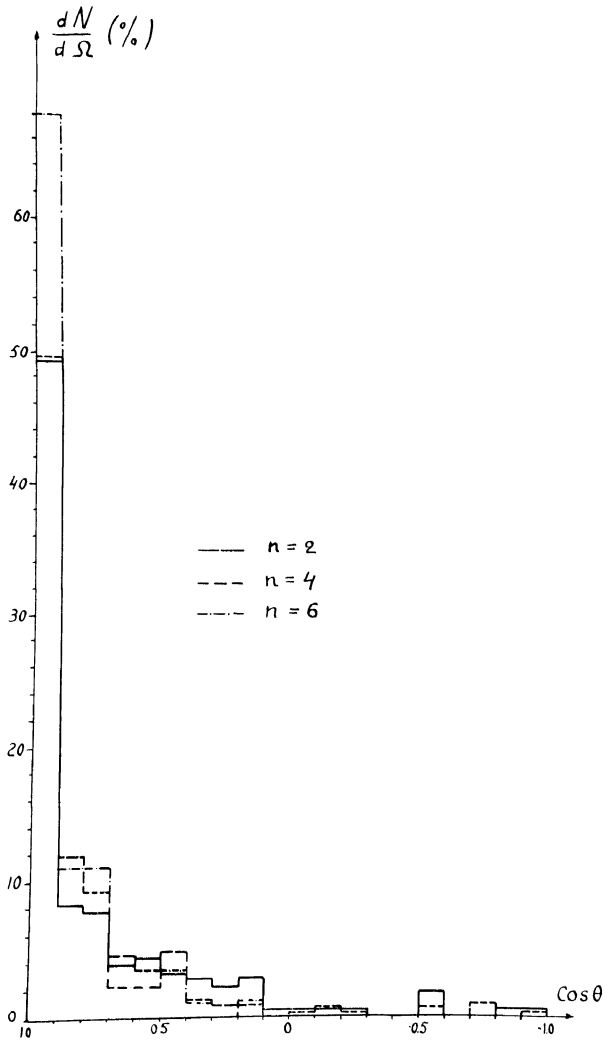
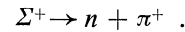


Fig. 2. The angular distributions of the secondary charged particles in  $p$ - $p$  collisions for the cases of different multiplicity ( $n$ ).

charged shower particles in  $p$ - $p$  and  $p$ - $n$  events are similar. They are in agreement qualitatively with calculations of the statistical theory<sup>16)</sup>. In Fig. 3 these distributions are compared with angular distribution for proton interaction with complex nucleus<sup>17)</sup>. In proton-nucleon collisions the secondary shower particles are concentrated in a narrower angle interval than in proton collisions with a complex nucleus. In particular, in the first case the ratio of forward-backward number of shower charged particles is  $39 \pm 8$ ; in the second case  $19 \pm 3$ . Such a difference in angular distributions (and in the mean number of fast charged particles) may be connected with cascade development inside the nucleus.

The tracks of all secondary particles from 115  $p$ - $p$  and 63  $p$ - $n$  events were followed either to rest, to their escape from the stack, to decay, or to secondary interaction. In  $p$ - $p$  events of 21 particle tracks stopped in the stack, 15 turned out to be protons and 6  $\pi$  mesons.

In  $p$ - $n$  events inside the stack 4 protons and 4  $\pi$  mesons stopped. One case of  $\Sigma^+$ -hyperon production in  $p$ - $p$  events was found, with decay according to the scheme



The mean free path for nuclear interaction of shower secondary particles from  $p$ - $p$  events is equal to  $(34 \pm 6)$  cm and from  $p$ - $n$  events  $(28 \pm 7)$  cm. These values do not differ from the mean free path for proton and  $\pi$  meson interactions with energy of 1 to 6 GeV, and from the preliminary range value for 9 GeV protons which were reported in paper<sup>17)</sup>. According to the data of the present paper the mean free range for 9 GeV proton interactions with nuclei in photo-emulsion is equal to  $(37.0 \pm 0.8)$  cm.

## B. Proton interaction with nuclei

### 1. Investigation of $\sim 9$ GeV proton interaction mechanism with photo-emulsion nuclei.

The interactions with light and heavy photo-emulsion nuclei have been separated from the stars, found by scanning along the track of incident protons. 53 stars on light nuclei and 67 on heavy ones have been selected for

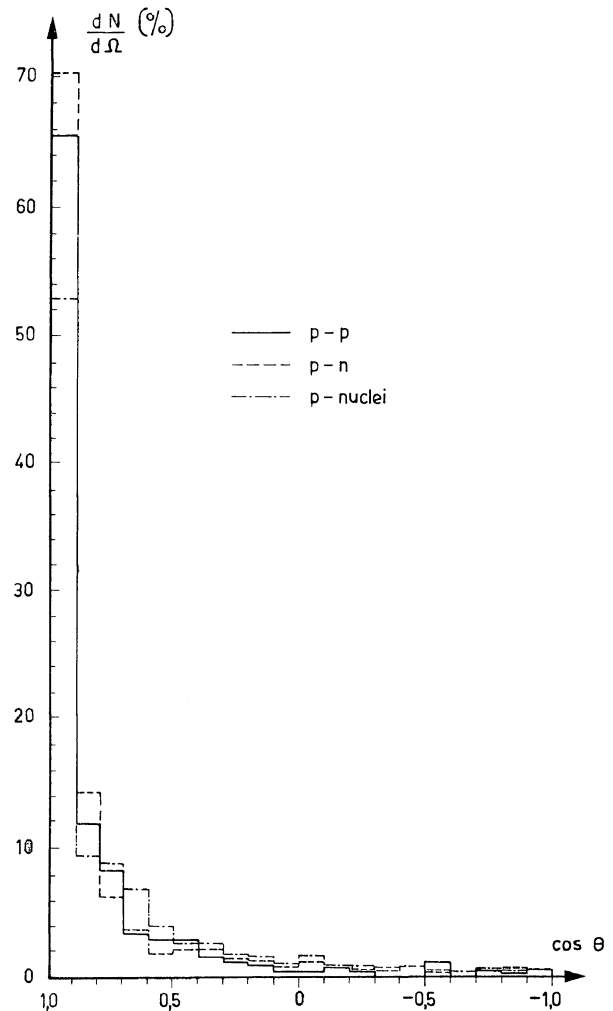


Fig. 3. The angular distributions of the charged shower particles in  $p$ - $p$ ,  $p$ - $n$  collisions and in proton collisions with photo-emulsion nuclei.

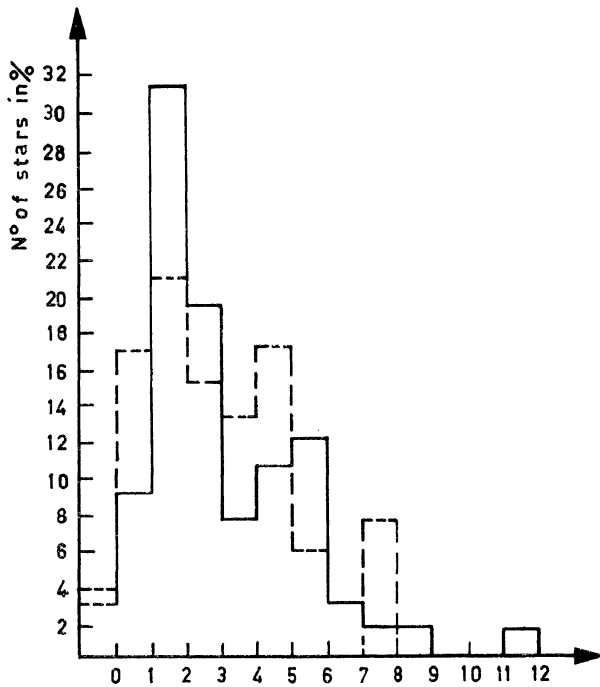


Fig. 4. Star distributions by the number of shower particles  $n_s$  on light and heavy nuclei. (—) heavy nuclei  $\bar{n}_s = 3.5 \pm 0.3$ ; (---) light nuclei  $\bar{n}_s = 3.4 \pm 0.3$ .

the analysis. All the prongs were divided into three classes according to the measurement of ionization :

1. shower particles (ionization  $I < 1.4 I_{plateau}$ );
2. grey particles (ionization  $I > 1.4 I_{plateau}$  and  $R > 3.73$  mm);
3. black particles (range  $R \geq 3.73$  mm, which corresponds to  $E = 30$  MeV protons).

Table II gives the mean values for shower, grey and black particles.

Star distribution by shower particles is given in Fig. 4.

The angular distributions of shower particles are given in Fig. 5. From the angular distributions the values of the median angles are obtained :

1. for  $p$ - $p$  collisions  $\theta_{1/2} = 18^\circ$  (is given for comparison)
2. for light nuclei  $\theta_{1/2} = 25^\circ$
3. for heavy nuclei  $\theta_{1/2} = 28^\circ$ .

The nuclear range for secondary interaction of shower particles obtained was  $34 \pm 6$  cm.

Fig. 6 gives the energy spectrum for grey particles.

The mean energy value per one particle and star was obtained :

	$\bar{E}_g$ MeV/prong	$\bar{E}_1$ MeV/star
light nucleus	$140 \pm 20$	$400 \pm 60$
heavy nucleus	$120 \pm 15$	$1160 \pm 120$

The median angles of grey particle angular distributions were estimated :

for  $p$ -light nuclei  $\theta_{1/2} = 57^\circ$ , for heavy nuclei  $\theta_{1/2} = 65^\circ$ . The mean black particle energy per star was determined by

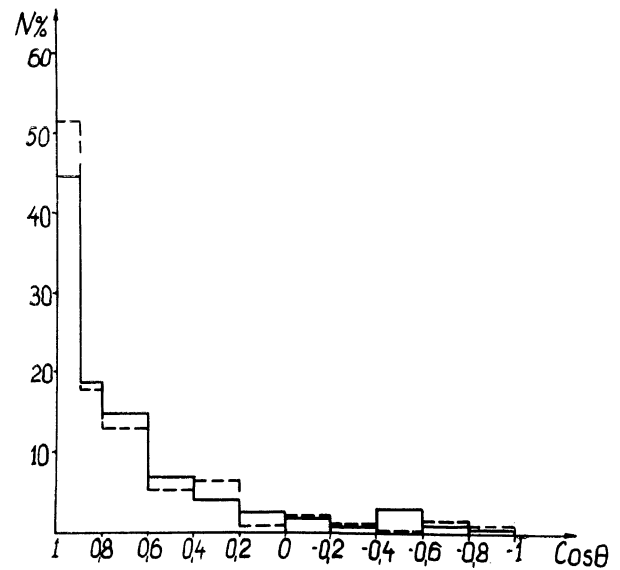


Fig. 5. The angular distributions of shower particles in the stars on light and heavy nuclei. (—) heavy nuclei  $\theta_{1/2} = 28^\circ$ ; (---) light nuclei  $\theta_{1/2} = 25^\circ$ .

TABLE II

Interaction type	Mean values		
	$n_s$	$n_g$	$n_b$
$p$ — light nuclei	$3.4 \pm 0.3$	$1.4 \pm 0.2$	$3.2 \pm 0.1$
$p$ — heavy nuclei	$3.5 \pm 0.3$	$4.1 \pm 0.5$	$6.1 \pm 0.6$
$p$ — mixture of nuclei	$3.2 \pm 0.2$	$3.1 \pm 0.4$	$4.7 \pm 0.5$

the values of the residual ranges of black tracks, taking into account binding energy and neutron emission in the disintegration of light and heavy nuclei :

for light nuclei  $\bar{E}_2 = 63 \pm 6$  MeV,

for heavy nuclei  $\bar{E}_2 = 245 \pm 25$  MeV.

From the results obtained the splitting energy of light and heavy nuclei was estimated :  $\bar{W} = \bar{E}_1 + \bar{E}_2$  :

$\bar{W}_{\text{light}} = 470 \pm 70$  MeV ;  $\bar{W}_{\text{heavy}} = 1400 \pm 120$  MeV.

The conclusion was made in the experiments on the cosmic rays that the average splitting energy of the air nucleus is  $440 \pm 160$  MeV at 3-40 GeV.

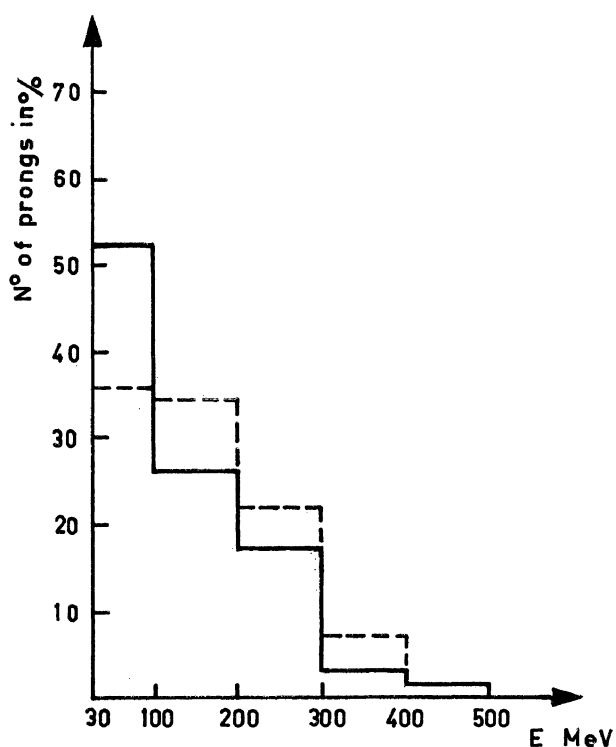


Fig. 6. The energy spectrum of grey prongs in the stars on light and heavy nuclei. (—) heavy nuclei  $\bar{E} = (122 \pm 12)$  MeV/prong,  $(1165 \pm 120)$  MeV/star; (---) light nuclei  $\bar{E} = (138 \pm 14)$  MeV/prong,  $(400 \pm 40)$  MeV/star.

An attempt was made to estimate primary particle energy losses for nuclear mixture, taking the average splitting energy of the mean photo-emulsion nucleus  $\bar{W} = 1050 + 110$  MeV and shower particle average energy  $\bar{E}_3$ . The energy value  $\bar{E}_3$  was obtained from the analysis of the secondary shower particle interactions by three angular intervals using dependence of  $n_s$  on the energy for  $\pi$  mesons and protons<sup>20)</sup>. The results are given in Table III.

According to the magnitudes  $\bar{W}$  and  $\bar{E}_3$  for the emulsion nucleus the average energy loss of the primary proton is  $(60 \pm \frac{25}{15})\%$ . We note for comparison that, using our average multiplicity of the mesons generated in the proton-nucleon collisions, and the average meson energy calculated theoretically<sup>21)</sup>, the energy loss in  $p$ - $p$  collisions is 40-50% and in paper<sup>19)</sup> the average energy losses on air nuclei appear to be equal to 30%.

Going from the angular distribution obtained for the shower particles (Fig. 5), the qualitative discussion of proton interaction mechanism with nuclei is now given. The extension of the median angle, observed in  $p$ -nucleus interaction in comparison with  $p$ - $p$  collisions, may be in agreement with the suggestion that in the light nuclei the proton is subject to 1.5 collisions, and in the heavy nuclei more than 2.

Table IV gives the calculated values of the median angles under the assumption of primary proton collision with different groups of nucleons (tube mechanism). The calculation is carried out assuming isotropy in c.m.s.

TABLE IV

Number of nucleons in the tube	$\theta_{1/2}$ under different assumptions on the average $\pi$ meson kinetic energy in c.m.s.		
	50 MeV	140 MeV	280 MeV
1	17°	22°	23°
2	24°	29°	32°
3	29°	35°	38°
4	33°	39°	42°

TABLE III

$\theta$	From secondary stars $\bar{n}_s$	$\bar{E}_p^*$	$\bar{E}^*$
0 - 10°	$1.4 \pm 0.4$	$5.2 \pm 1.7$	$4.0 \pm \begin{smallmatrix} 0.6 \\ 0.9 \end{smallmatrix}$
10 - 20°	$0.7 \pm 0.3$	$1.8 \pm 1.5$	$2.2 \pm \begin{smallmatrix} 0.9 \\ 1.4 \end{smallmatrix}$
20 - 180°	$0.35 \pm 0.15$	—	$0.5 \pm \begin{smallmatrix} 0.9 \\ 0.3 \end{smallmatrix}$

Note :  $\bar{E}_p^*$ ,  $\bar{E}^*$  — effective energy, if secondary particles are protons or  $\pi$  mesons.

Table IV shows that the tube dimensions can be chosen so that the experimental values are in accordance with calculation. However, the calculated values were obtained assuming that the mesons generated in the collision do not interact with nucleons, which contradicts our experimental data on the number of the grey particles and on the splitting energy of the nuclei. Besides that, considerable extension of the angular distribution of the shower particles due to the meson interaction inside nuclei must follow from the value of the average of the nuclear range and the angular distribution. Thus, by meson-nucleon collisions, the co-ordination of the tube model seems to be more complicated with our data than the model of nucleon-nucleon collision.

## 2. Generation of $\pi^0$ mesons at $\sim 9$ GeV proton interaction with photo-emulsion nuclei.

To study the interaction mechanism of the high energy particles the question about the rate of energy transfer to the secondary  $\pi$  mesons is of great interest.

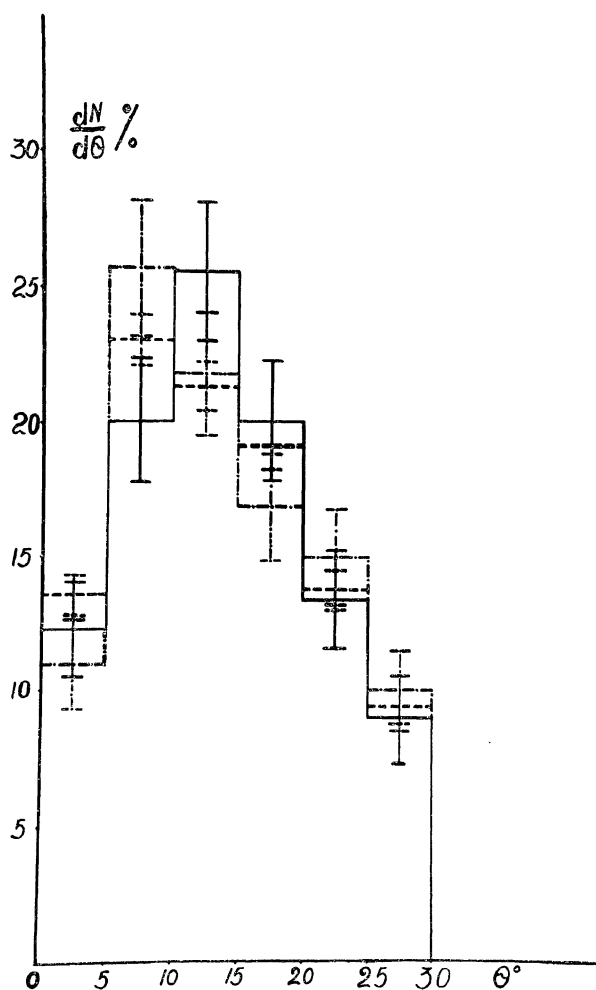


Fig. 7. Emitted angular distribution of electron-positron pairs (—) and angular distribution of shower particles from stars, found at the scanning along the tracks of primary protons (---) and from the stars, found at the scanning of secondary shower particles (-.-.-).

Because the direct measurement of fast charged  $\pi$  meson energy in photo-emulsion is rather complicated, the average energy of  $\gamma$ -quanta due to  $\pi^0$  meson decay was estimated. For this purpose, electron-positron pairs induced by  $\gamma$ -quanta were searched. The pairs were found by scanning of separate relativistic tracks.

The tracks with plane angle relative to the beam direction  $1^\circ < \varphi < 30^\circ$  and the projected length in one plate  $l \geq 1600 \mu$  were chosen. The chosen tracks were followed back to the generation point of the pair, star or escaping point from the stack. Similar scanning of the pairs was proposed by King<sup>22)</sup>. It is suitable for our work because it excludes the possible bias of the pairs by the energies. Excluding the inconsiderable background due to Bremsstrahlung  $\gamma$ -quanta, and  $\gamma$ -quanta incident on the stack from the outside, the number of pairs found was 93, and the number of the relativistic tracks leading to the stars was 116. In both cases the distributions of angles with respect to the beam are given in Fig. 7. The angular distribution of shower particles in stars, found by scanning along the tracks of the primary protons, was also found. All the distributions coincide within the error limits. Since in the interval of the investigated energies the angular distributions of  $\gamma$ -quanta and  $\pi^0$  mesons are approximately the same, one may consider that the angular distributions of neutral and charged  $\pi$  mesons are also close to each other.

The estimation of  $\gamma$ -quantum average energy can be made by the distribution of angles between pair components, because

$$\bar{E}_\gamma = K \left( \frac{1}{\omega} \right).$$

The calculations, based on the data<sup>23)</sup> and<sup>24)</sup>, show that  $K = 4.15$ , if the angles are expressed in radians and the energy in MeV.

The measurements of the angular separation were carried out by the method proposed in<sup>25)</sup>, which reduces the influence of the multiple scattering. The mean value of  $\gamma$ -quanta energy is  $\bar{E}_\gamma = 420 \pm 100$  MeV.

The given error includes the measurement error, inaccuracy in the determination of the coefficient  $K$ , approximation inaccuracy and statistical error in determination of  $\left( \frac{1}{\omega} \right)$ .

To transit to the average energy of  $\pi^0$  mesons the ratio of  $f = \bar{E}_{\pi^0} / \bar{E}_\gamma$  must be estimated. The magnitude depends on the type of  $\pi^0$  meson energy spectrum, but this dependence is rather weak. The upper limit of  $f$  value under reasonable assumptions on  $\pi^0$  meson spectrum equals 1.8. Therefore, the upper limit of the average  $\pi$  meson energy equals  $(750 \pm 180)$  MeV.

The total energy, transmitted to the all  $\pi^{0\pm}$  mesons is

$$\bar{E}_\pi = 3/2 (\bar{n}_s - a) \bar{E}_{\pi^0},$$

where  $a$  is the average number of the secondary relativistic protons. For proton interaction of the considered energy

with photo-emulsion nuclei  $\bar{n}_s$  equals  $3.4 \pm 0.1$ . If one considers all the shower particles as  $\pi$  mesons then  $\bar{E}_\pi = 3.8$  GeV.

One should bear in mind that the obtained value  $\bar{E}_\pi$  relates not to all  $\pi$  mesons but only to those which emit in the limits of the solid angle considered. Further, in the calculation one should take into account the presence of the protons among the relativistic particles.

These two considerations lead to reduction of the  $\bar{E}_\pi$  value. On the other hand, the energy connected with black and grey prongs (generally with split nuclei) is partially due to  $\pi$  meson energy and it increases  $\bar{E}_\pi$ . The accurate account of the influence of all facts mentioned has not yet been done. In any case, one may think that the energy share of the primary protons transferred to mesons is less than 50%. The total energy losses (including  $\delta$ -nucleon production) may be greater.

### 3. Generation of strange particles at 9 GeV proton collisions with photo-emulsion nuclei.

To detect hyperons and  $K$  mesons the tracks of secondary single charge particles produced in nucleus interactions induced by primary protons have been investigated. The mentioned tracks were followed to the rest point, decay, nuclear interaction or to escape from the stack.

The selection of strange particles was made by the decay scheme and nuclear capture. Only the particles which emitted in the forward hemisphere and which satisfied the following two conditions were followed:

- a) The ionisation exceeded that of primary protons not less than 1.6 times ( $\beta \leq 0.64$ );
- b) the projected length in one pellicle  $\geq 3$  mm, which corresponds to the dip. angle  $\leq 7.5^\circ$ .

This last condition excluded also the majority of slow protons and deuterons produced by evaporation from excited nuclei.

The results of 670 followed tracks from 1920 stars are given in the Table V.

Thus, under the conditions considered, one strange particle is approximately produced per 130 secondary particles. The great value of the ratio of the number of strange particles to the number of  $\pi$  mesons

$$(N_{\Sigma, K} | N_\pi) \approx 1/4$$

is striking.

In addition to 5 mentioned strange particles, 25 strange particles were found during the scanning along the area, most of which were produced in stars induced by primary protons. The data relating to all found particles are given in Table VI. Only in one case a strange particle was found ( $K^\pm$  meson), which was emitted backwards. In the reaction  $N + N \rightarrow \Sigma + K + N$  the maximal emergence angle of  $\Sigma$  is  $44^\circ$ . Out of the

9  $\Sigma$ -particles found, 4 emerge under considerably greater angles. This circumstance probably should be connected with the secondary hyperon interactions with nucleons of the parent nucleus.

The stars induced by the primary protons and containing slow strange particles possess a higher number ( $N_h$ ) of grey and black tracks. In fact, for this group of the stars we have  $\bar{N}_h = 12.9 \pm 1.6$  and  $\bar{n}_s = 3.3 \pm 0.5$ , while for the usual stars induced by primary protons  $\bar{N}_h = 8.3 \pm 0.5$  and  $\bar{n}_s = 3.4 \pm 0.1$ <sup>17)</sup>.

An analogous phenomena was mentioned in some other papers. For example in the work<sup>20)</sup> carried out on  $\pi$  mesons ( $E_\pi \sim 4.3$  GeV) for the stars containing strange particles,  $\bar{N}_h = 11.5 \pm 0.5$  and  $\bar{n}_s = 0.9 \pm 0.1$ , compared with the usual values  $\bar{N}_h = 6.5 \pm 0.6$  and  $\bar{n}_s = 1.7 \pm 0.1$

In the stars containing strange particles all prongs were followed. The associated production was found in three cases, in one of which two  $K$  mesons were produced.

Assuming that the ratio between the number of strange particles and usual ones does not depend strongly on the emergence angle, a rough estimation of the generation cross-section of charged strange particles with velocity  $\beta \leq 0.64$  on photo-emulsion nuclei can be given: per one nucleon  $\sigma_{\Sigma, K} \sim 0.5$  mb.

### 4. On the possibility of investigating the 9 GeV proton diffraction scattering on nuclei.

The investigation of elastic scattering of great energy particles on nucleons and on nuclei is a suitable method to study their structure, since under these conditions the quasi-classical approximation turns out to be valid. Unfortunately, the experiments demand a measurement of very small scattering angles.

The method considered allows the investigation of angular distributions up to angles  $\sim 0.2^\circ$  in a way analogous to the measurements of the multiple scattering. In this connection the distances of the track of the primary proton from some fixed straight line (viz. direction of the microscope stage) were measured at various points, and this enabled the dip angle and the scattering angle to be determined.

In the described methods of searching and measurements of small angle scatterings the main shortcoming of the usual scanning along the track, under which the efficiency of scattering detection depends on the angle, is absent.

On the other hand, one should not undertake the search for point scatterings, but should compare the angular distributions of the primary beam obtained in different places of the photoplate, i.e. after going through various thicknesses of photo-emulsion.

The comparison of these distributions gives a possibility of experimentally checking the different assumptions on the character of nuclear scattering.

TABLE V

The total number of tracks	The track number without visible phenomena at rest	$\pi$ meson number	Strange particles number	The secondary interaction number	The track number escaped from the stack
670	474	19	5	53	97

TABLE VI

$NN$	Particle type	Parent star type	Particle energy MeV	The angle between the emergence direction and the primary proton	Remarks
1	2	3	4	5	6
1.	$K^+$	$5 + 3 p$	50		Associated with No. 21. Associated with No. 22.
2.	$K^+$	$22 + 3 p$	108		
3.	$K^+$	$14 + 7 p$	62		
4.	$\Sigma^-$	$4 + 3 p$	218	$42^\circ$	
5.	$\Sigma^\pm$	$21 + 1 p$	$\sim 97$	$82^\circ$	
6.	$K^+$	escapes the stack			Associated with No. 29.  $\Lambda^0$ -particle decayed at $\sim 200\mu$ from generation point that permitted determination of the parent star type.
7.	$K^+$	$4 + 4 p$	20		
8.	$K^+$	$7 + 0 n$	110		
9.	$K^+$	$4 + 0$ charged	110		
10.	$K^+$	$6 + 5 p$	87		
11.	$K^+$	$21 + 4 p$	60		
12.	$K^+$	$3 + 0$ charged	50		
13.	$K^+$	$7 + 9 p$	30		
14.	$K^+$	$11 + 1 p$	52		
15.	$K^+$	escapes the stack			
16.	$K^+$	$21 + 0 p$	75		
17.	$K^+$	escapes the stack			
18.	$K^+$	$6 + 1 p$	97		
19.	$\Sigma^\pm$	$18 + 5 p$	$> 14$	$89^\circ$	
20.	$\Sigma^+$	$12 + 4 p$	35	$90^\circ$	
21.	$\Sigma^+$	$5 + 3 p$	$\sim 800$	$20^\circ$	
22.	$\Sigma^-$	$22 + 3 p$	115	$29^\circ$	
23.	$\Sigma^\pm$	$14 + 1 p$	$> 145$	$91^\circ$	
24.	$Hf$	$27 + 3 p$	—		
25.	$Hf$	$11 + 4 p$	—		
26.	$\Lambda^0$	$18 + 2 p$	140		
27.	$\Lambda^0$	—	109	—	
28.	$\Lambda^0$	—	19		
29.	$K^+$	$6 + 1 p$	106		
30.	$\Sigma^\pm$	$8 + 0 n$	$\geq 38$		
31.	$\Sigma^\pm$	$2 + 1 n$	60	$36^\circ$	

This method can be used with some modification for the investigation of the scattering not only by the photo-emulsion nuclei but also by the nuclei of any other material.

Due to the great distortion of photo-emulsion the angles were measured by a relative method. Pairs of primary protons spaced from each other not more than 50-60  $\mu$  were chosen for this purpose.

To compare the projected angle distributions between the particle pairs the measurements at the depth of 5 mm and 95 mm from the edge of the emulsion stack, faced to the beam, were made. About 1200 track pairs were measured in such a way.

The distributions obtained are given in Figs. 8 and 9. It is necessary to take into account the influence of multiple Coulomb scattering in emulsion for their comparison.

The angular distribution at 95 mm allowing only for Coulomb multiple scattering is given in Fig. 9. The difference between this distribution and the experimentally measured one at 95 mm must be considered to be due to the influence of nuclear scattering.

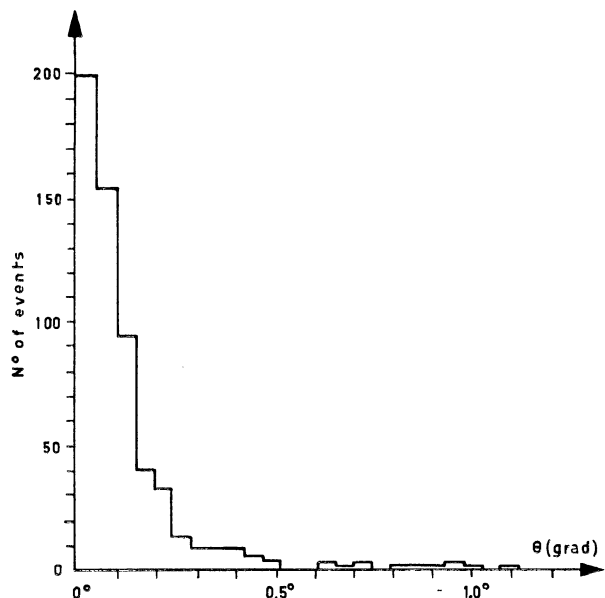


Fig. 8. Distribution of projected angles of the primary protons at the depth of 5 mm.

As is seen from Fig. 9 the statistics allow only rough analysis. Therefore, the model of the "black sphere" was chosen as the first approximation and the radius of the nuclei contained in the emulsion was assumed to be equal to

$$R_i = r_0 A_i^{1/3} .$$

The value  $r_0 = 1.25 \cdot 10^{-13}$  cm was determined from the mean path for inelastic interaction in photo-emulsion equal to  $(34.7 \pm 1.5)$  cm (see <sup>17</sup>).

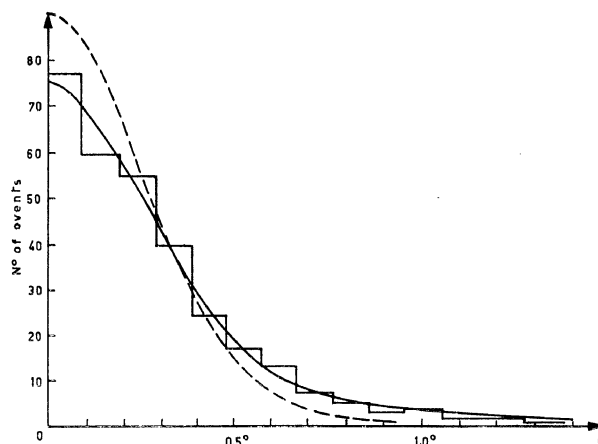


Fig. 9. Distribution of projected angles of the protons at the depth of 95 mm. (—) smooth curve = expected distribution calculated by black sphere model, (---) = expected angular distribution obtained allowing only for Coulomb multiple scattering.

The angular distribution, calculated taking into account the nuclear scattering by the "black sphere" model, is given as the lower curve in Fig. 9, and is in a good agreement with experimental data.

When using the second of the above described methods, the angles between track pairs in two points spaced at a distance of 1 cm were measured. If this angle changed more than 0.2°, repeated measurements of the angle after every 2 mm were made.

In such a way 1132 pairs were investigated (the total length of tracks is 22 m) and 31 scattering cases at the angle  $> 0.3^\circ$  were found. The corresponding angular distribution and that calculated by the "black sphere" model are plotted in Fig. 10.

The "black sphere" model provides 24 scatterings, which within the error limits are in agreement with the experiment. The results obtained must be considered as preliminary.

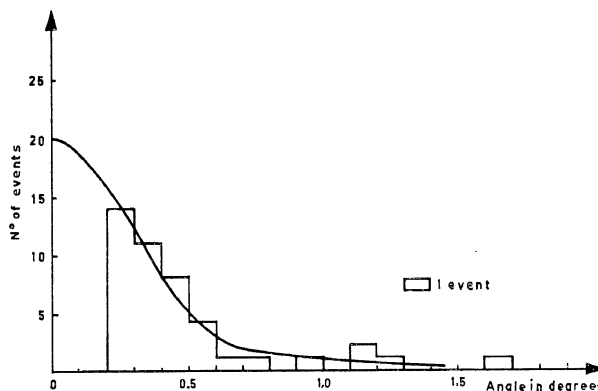


Fig. 10. Distribution of projected angles for 44 scattering cases on the angle 0.2°. Smooth curve = expected distribution calculated by "black sphere" model.

## LIST OF REFERENCES

1. Rodicheva, M. F. (to be published in Zhurnal nauchnoj i prikladnoj fotografii i kinematografii)
2. Bradna, F. G. and Kriventsova, L. G., Report, Joint Institute for Nuclear Research, Dubna, 1958.
3. Bogachev, N. P. Doklady Akad. Nauk, SSSR, *103*, p. 806, 1956.
4. Dzhelepov, V. P., Moskalev, V. I. and Medved', S. V. Doklady Akad., Nauk, SSSR, *104*, p. 380, 1955.
5. Fowler, W. B., Shutt, R. P., Thorndike, A. M., Whittemore, W. L., Cocconi, V. T., Hart, E., Block, M. M., Harth, E. M., Fowler, E. C., Garrison, J. D. and Morris, T. W. Phys. Rev., *103*, p. 211, 1956.
6. Chen, F. F., Leavitt, C. P. and Shapiro, A. M. Phys. Rev., *103*, p. 1489, 1956.
7. Smith, L. W., Mc Reynolds, A. W. and Snow, G. Phys. Rev., *97*, p. 1186, 1955.
8. Duke, P. J., Lock, W. O., March, P. V., Gibson, W. M., Mc Ewen, J. G., Hughes, I. S. and Muirhead, H. Phil. Mag., *2*, p. 204, 1957.
9. Hughes, I. S., March, P. V., Muirhead, H. and Lock, W. O. Phil. Mag., *2*, p. 215, 1957.
10. Cork, B., Wenzel, W. A., and Causey, C. W. Phys. Rev., *107*, p. 859, 1957.
11. Cester, R., Hoang, T. F. and Kernan, A. Phys. Rev., *103*, p. 1443, 1956.
12. Wright, R. W., Saphir, G., Powell, W. M., Maenchen, G. and Fowler, W. B. Phys. Rev., *100*, p. 1802, 1955.
13. Begzhanov, R. B. Zh. eksper. teor. Fiz., *34*, p. 775, 1958.
14. Alekseeva, K. I. and Grigorov, N. L. Doklady Akad., Nauk, SSSR, *117*, p. 593, 1957.
15. Brenner, A. E. and Williams, R. W. Phys. Rev., *106*, p. 1020, 1957.
16. Barashenkov, V. S. (private communication)
17. Bogachev, N. P., Van Shu-fen', Gramenitskij, I. M., Kirillova, F. L., Lebedev, R. M., Lyubimov, V. B., Markov, P. K., Merekov, Yu. P., Podgoretskij, M. I., Sidorov, V. M., Tolstov, K. D. and Shafranova, M. G. Atomnaya Energiya, *4*, p. 281, 1958.
18. Barashenkov, V. S. et al. (private communication of V. S. Barashenkov)
19. Vernov, S. N., Grigorov, N. L., Zatsepin, G. T. and Chukadov, A. E. Izv. Akad. Nauk, SSSR, Ser. Fiz., *19*, p. 493, 1955. Grigorov, N. L. Dissertation, Moscow University, 1954.
20. Lock, W. O. and March, P. V. Proc. Roy. Soc. A., *230*, p. 222, 1955. Johnson, W. R. Phys. Rev., *99*, p. 1049, 1955. Blau, M. and Caulton, M. Phys. Rev., *96*, p. 150, 1954. Walker, W. D. and Crussard, J. Phys. Rev., *98*, p. 1416, 1955. Cavanaugh, R. E., Haskin, D. M. and Schein, M. Phys. Rev., *100*, p. 1263, 1955.
21. Barashenkov, V. S. (private communication)
22. King, D. T. (private communication)
23. Heitler, W. Quantum theory of radiation. 3rd. ed. Oxford, Clarendon Press, 1954.
24. Borsellino, A. Phys. Rev., *89*, p. 1023, 1953.
25. Weill, R., Gailloud, M. and Rosselet, Ph. Nuov. Cim., *6*, p. 413, 1957.
26. Besson, C., Crussard, J., Fouché, V., Hennessy, J., Kayas, G., Parikh, V. R. and Trilling, G. Nuov. Cim., *6*, p. 1168, 1957.